Compumag 2011

12 - 15 July 2011, Sydney, Australia

18th International Conference on the Computation of Electromagnetic Fields

(www.compumag2011.com)

TECHNICAL PROGRAM

(Draft on 22 June 2011)

PC10.6 (ID 752)
Characteristics Analysis of Single Phase Induction Motor by Equivalent Circuit Method Considering Saturation Factor
Cho, SuYeon; Ham, SangHwan; Jang, IkSang; Ryu, GwangHyeon; Kim, MiJung; Lee, Ju
Hanyang University, Korea, South (Republic of)

PC10.7 (ID 753)
Characteristic Analysis on PMSMs with Three Types of Diametrically Magnetized Rotors under Magnetic Circuit Construction Conditions
Jang, Seok-Myeong (1); Koo, Min-Mo (1); Park, Yu-Seop (1); Choi, Jang-Young (1); Lee, Sung-Ho (2)
1: Chungnam National University, Korea, South (Republic of); 2: Korea Institute of Industrial Technology, Korea, South (Republic of)

PC10.8 (ID 755)
A Study on the Simulated Torque Table with Nonlinear Datasets of IPMSM for HEV
Kim, Won-Ho; Jin, Chang-Sung; Jang, Ik-Sang; Kim, Mi-Jung; Lee, Ki-Doek; Lee, Ju
Hanyang Univ., Korea, South (Republic of)

PC10.9 (ID 759)
Optimal Shape Design of Rotor Bar of Three-phase Squirrel Cage Induction Motor for NEMA Design D Torque-speed Characteristics
Koh, C. S. (1); Zhang, Dianhai (1); Li, Wei (1); Park, Chang Soon (2)
1: Chungbuk National University, Korea, South (Republic of); 2: Korea University of Technology and Education, Korea, South (Republic of)

PC10.10 (ID 761)
Numerical Investigation on Torque Harmonics Reduction of Interior Permanent Magnet Synchronous with Concentrated Winding
Lee, Seungho; Lee, Dongsu; Kim, Yong-Jae; Jung, Sang-Yong
Dong-A Uni., Korea, South (Republic of)

PC10.11 (ID 762)
Electro-magnetic Losses Calculation and Reduction of High-speed Permanent Magnet Synchronous Motor using Measured Load Current Waveform with Harmonics and 2-D FEM
Jang, Seok-Myeong (1); Han, Cheol (1); Choi, Jang-Young (1); Lee, Yong-Bok (2)
1: Chungnam national university, Korea, South (Republic of); 2: Korea Institute of Science and Technology, Korea, South (Republic of)

PC10.12 (ID 764)
Research on the Electromagnetic Performance of an Axial Flux Permanent-Magnet Linear Synchronous Machine
Zheng, Ping; Tong, Chengde; Gan, Xuhui; Sui, Yi; Ke, Wenjing; Yan, Haiyuan
Harbin Institute of Technology, China, Peoples Republic of

PC10.13 (ID 768)
Permanent Magnet Temperature Estimation of IPMSM using Thermal Equivalent Circuit
Lee, Byeong-Hwa (1); Kim, Kyu-Seob (1); Song, Baik-Kee (1); Sun, Tao (1); Hong, Jung-Pyo (1); Kim, Young-Kyoun (2)
1: Hanyang University, Korea, South (Republic of); 2: Korea Electronics Technology Institute, Korea, South (Republic of)

Temperature Estimation of IPMSM using Thermal Equivalent Circuit

Byeong-Hwa Lee[1], Kyu-Seob Kim[1], Tao-Sun[1], Jae-Woo Jung[1], Jung-Pyo Hong[1], *Senior member, IEEE* and Young-Kyoun Kim[2]
[1]Department of Automotive Engineering, Hanyang University, Haengdang-dong, Seongdong-gu, Seoul, 133-791, Korea
[2]Korea Electronics Technology Institute, Yatap-Dong, Wonmi-gu, Bucheon, Gyeonggi-do, 420-733, Korea

This paper deals with the temperature estimation of interior permanent magnet synchronous motor (IPMSM). A thermal equivalent circuit of IPMSM considering eddy current loss of PM and core losses of rotor is proposed. And the transient 3D finite element analysis is used to calculate the eddy current loss of PM. This thermal equivalent model is represented by the thermal resistances and thermal capacitances. In order to determine the factor of these components, a heating test is processed. Finally, this thermal equivalent model is verified by a temperature test in a 25kW 12-pole/18-slot IPMSM.

***Index Terms*—Interior permanent magnet synchronous motor, Demagnetization, Eddy current loss, Permanent magnet temperature estimation, thermal equivalent circuit,**

I. Introduction

Interest in interior permanent magnet synchronous machines (IPMSM) has been growing for several years at various fields, such as industry, home appliance, and transportation [1]-[3]. In the design of IPMSM, the thermal is highly constrained with specified electromagnetic torque and power because of the temperature sensitive materials. For example, the knee point of NdFeB magnet rises as the temperature increases. Thus the irreversible demagnetizing might occur at high temperature [4], [5]. In the design of IPMSM, therefore, it is necessary to estimate the PM temperature of the IPMSM in order to guarantee that it is near the designed value as well as the total temperature.

In order to estimate the temperature of IPMSM, in this paper, a thermal equivalent circuit for the totally enclosed structure is proposed. Not only can it be used to solve the steady-state temperature, but also suitable for estimating the transient temperature. It is described with the dimensions of each motor components and constant thermal coefficients, which means that it is adaptive to various models. In addition, it is different from the conventional thermal model, an extra thermal model for eddy current loss of PM is considered, which increases the calculation accuracy of this model. Compared with finite element analysis (FEA), the solving process of this thermal equivalent circuit spends shorter time. And it can show the temperature of each component of IPMSM, such as the tooth, yoke, PM and so on. Therefore, it will be a very effective method to estimate the temperature of IPMSM in the design process.

This paper first introduce the fundamental theory on the equivalent circuit of thermal including the thermal resistance modeling, thermal capacitance modeling, and thermal equivalent circuit networking. Then, a numerical method on the loss calculation be presented. A heating test is processed to determine the thermal coefficients. Finally, the temperature of a 25kW IPMSM which is applied in an in- wheel EV traction system is estimated and measured by the proposed equivalent thermal model and an experiment in order to verify the validation.

Manuscript received May 30, 2010.
Corresponding author: Jung-Pyo Hong (e-mail: hongjp@hanyang.ac.kr).
Digital Object Identifier inserted by IEEE

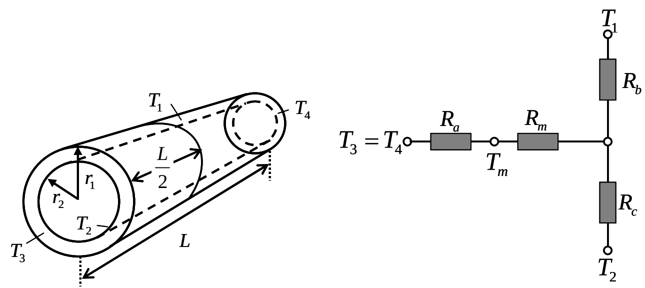

Fig. 1. General Cylindrical component: (a) Cylindrical model (b) Thermal network for symmetric component

II. Principle of Thermal Equivalent Circuit

A. General Cylindrical Component of Mellor and Turner

A general cylindrical symmetric model as shown in Fig. 1.(a) is studied in this paper. The corresponding elementary network proposed by Mellor and Turner is shown in Fig 1. (b) [6]. In Fig. 1 (b), the resistance R_a represents the thermal conduction resistance in the axial direction, while R_m, R_b and R_c represent the thermal conduction resistance in the radial direction. These resistances are defined in terms of the dimensions of the cylinder, and the axial and radial thermal conductivities, k_a and k_r as expressed in (1)-(4).

$$R_a = \frac{L}{6\pi k_a (r_1^2 - r_2^2)} \tag{1}$$

$$R_b = \frac{1}{2\pi k_r L}\left[1 - 2r_2^2 \ln\left(\frac{r_1}{r_2}\right) / (r_1^2 - r_2^2)\right] \tag{2}$$

$$R_c = \frac{1}{2\pi k_r L}\left[2r_1^2 \ln\left(\frac{r_1}{r_2}\right) / (r_1^2 - r_2^2) - 1\right] \tag{3}$$

$$R_m = \frac{-1}{4\pi(r_1^2 - r_2^2)k_r L}\left[(r_1^2 + r_2^2) - 4r_1^2 r_2^2 \ln\left(\frac{r_1}{r_2}\right) / (r_1^2 - r_2^2)\right] \tag{4}$$

B. Thermal Resistance and Capacitance Modeling

The Mellor and Turner model is proposed for the Induction motor [7], [8]. Based on their previous works, a new thermal network for the IPMSM is proposed in this paper. In this thermal equivalent circuit, the resistance of the motor is divided into nine parts: frame, stator yoke, stator teeth, end winding, slot winding, air gap, end cap air, rotor and shaft. And rotor part consists of outer rotor, magnet, flux barrier tip and inner rotor. Fig. 2 and Fig. 3 show the equivalent rotor structure and the components of thermal equivalent circuit of IPMSM. Under the high speed, core loss of rotor and eddy current loss of magnet are distributed at outer rotor and magnet, respectively. Therefore, these components are modeled separately. The thermal resistances of these four components of rotor part are calculated by equation (1)-(4).

And the convective heat transfer between the exposed surfaces of the solid components and the internal or external cooling air are modeled in the usual manner by a single thermal resistance R_c, which has a value equal to the reciprocal of the surface area A_c in contact with the cooling air times a boundary film coefficient h [6].

$$R_c = \frac{1}{hA_c} \tag{6}$$

These two cases are denoted by the subscripts.

(i) h_1 : heat transfer between frame and external air
(ii) h_2 : heat transfer between stator or rotor and air gap

h_1 is a natural convective heat transfer coefficient that is determined empirically. h_2 is forced convective heat transfer coefficient that is calculated by the air gap between the stator and rotor.

$$h_2 = \frac{N_{Nu} k_{air}}{l_g} \tag{7}$$

where the *Nusselt* number N_{Nu} for the convective heat transfer between two rotating smooth cylinders is given by Taylor. The expression of *Nusselt* numbers for the small air gap machines in *Taylor* is

$$N_{Nu} = 2.2 \quad N_{Ta} \leq 41 \tag{8}$$

$$N_{Nu} = 0.23 N_{Ta}^{0.63} N_{\mathrm{Pr}}^{0.27} \quad 41 < N_{Ta} \leq 100 \tag{9}$$

where the dimensionless *Taylor* N_{Ta} and *Prandtl* numbers N_{pr} are defined from the air gap dimensions and fluid constants using the expressions given by Taylor. The critical value of 41 form the *Taylor* number refers to a change from laminar flow, which is normal in small air gapped machines, to turbulent flow.

The total thermal capacitance of the cylinder is found from the material density ρ, the specific heat c_p and the motor dimensions as

$$C = \rho c_p \pi (r_1^2 - r_2^2) L \tag{10}$$

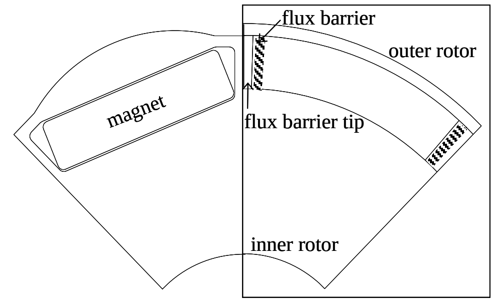

Fig. 2. Equivalent rotor structure for thermal analysis

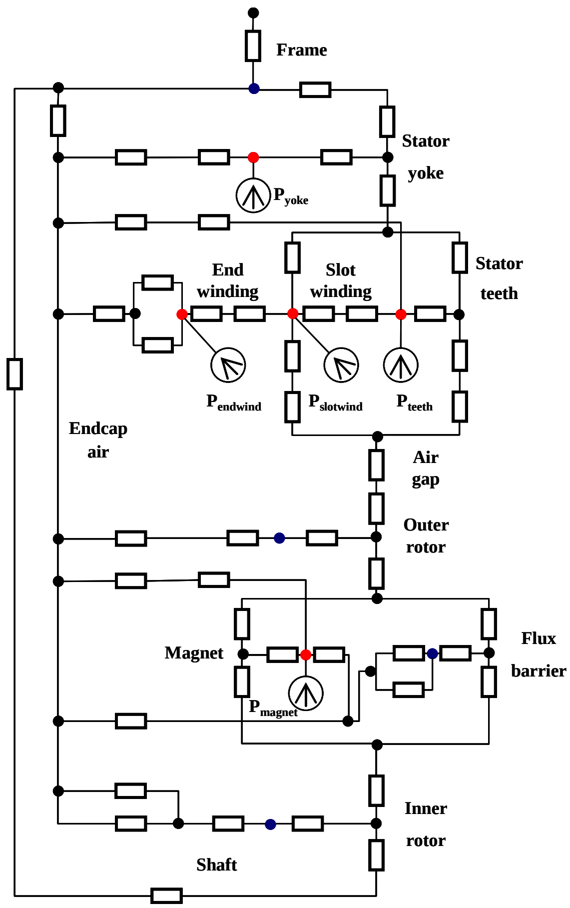

Fig. 3. Equivalent rotor structure for thermal analysis

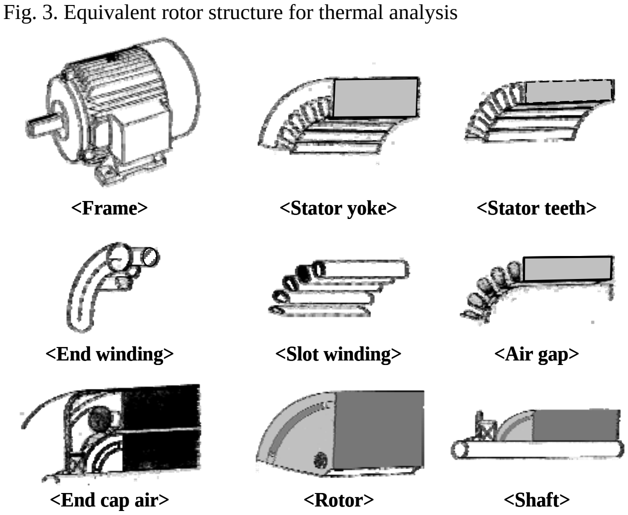

Fig. 4. Component of equivalent circuit

C. Loss Modeling

- Eddy current loss

In order to reduce the eddy current loss, the cores of stator and rotor are laminated by the thin electric steel. Different to the laminated core, the permanent magnet usually has single body or few segments due to manufacture and cost issue. Therefore, the eddy current loss in PM is much larger than the core of rotor, and even might be larger than the copper loss of armature winding at high speed operation region. The eddy current loss directly causes the temperature of magnet increases and the total efficiency of motor decreases. It is necessary to consider it in the equivalent thermal circuit. In this paper, the eddy current loss of PM is calculated in transient 3D FEA [9].

- Iron loss

Fig. 4 shows the flow chart for the core loss calculation [10], [11]. The temporal and the spatial variations of the magnetic flux density waveforms are calculated by electromagnetic FEA. Spectrum analysis is used for the frequency analysis of the magnetic flux density at each element of the FEA model. Core-loss data provided by manufacture are described with frequency and flux densities. Under sinusoidal flux conditions, core loss is computed in the frequency domain.

D. Thermal Equivalent Circuit

The thermal equivalent circuit network of IPMSM is shown in Fig. 3. Supposing constant thermal capacitance and resistance in every node, a linear differential equation for the node i can be derived as expressed in (5).

$$C_i \frac{dT_i}{dt} = \frac{1}{R_{ji}}(T_j - T_i) + g_i \qquad (5)$$

where C_i is the i^{th} node thermal capacitance, T_i is the i^{th} node temperature, R_{ji} is thermal resistance between two adjacent node i and j.

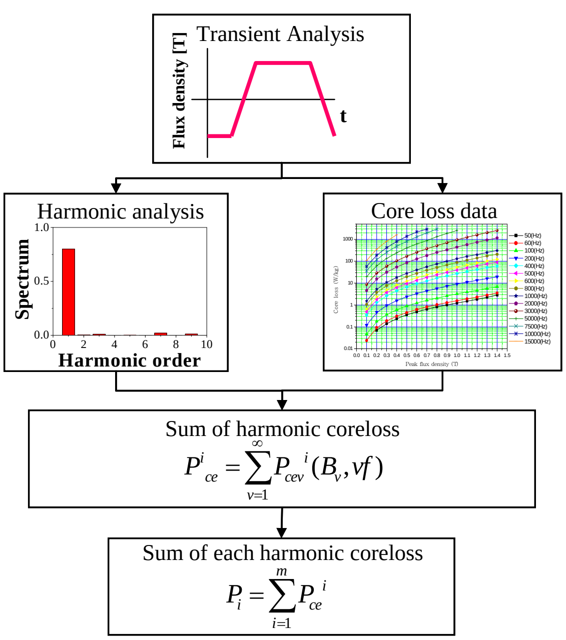

Fig. 6. Calculation process of core loss

III. Performance of Thermal Model

A. Analysis model

The thermal model in the article model is IPMSM for in-wheel type electric vehicle. Table I shows specifications. Output characteristics are shown in Fig. 4. In the constant torque region, MTPA control is applied to and field weakening control is applied in constant power region. Rotor and stator structure are shown in Fig.4.

B. Analysis results

The loss of motor is shown as TABLE II. After teeth, yoke and rotor are separated respectively, core loss is computed according to speed and flux density calculated by FEA. Room temperature of 25 degree was assumed. Finally, thermal equivalent circuit is analyzed by using calculated values and the result is shown in Fig.9. The temperatures of End-coil, housing, frame and permanent magnet is estimated. As a result of analysis, end-coil is saturated at 148 degree which is the highest temperature, permanent magnet at 85.9 degree, housing at 79.8 degree and motor flange at 70.9 degree respectively.

TABLE I
Specification of Analyzed and Tested IPMSM for In-Wheel Applicationl

Specification	Values
Pole / Phase number	12 / 3
Rated output power	10 kW
Base speed / Max. speed	1250 / 5000 rpm

TABLE II
Core Loss and Eddy Current Loss

	Core loss [W]				Eddy current loss [W]
	Total	Tooth	Yoke	Rotor	
1250rpm	94.3	38.4	40.6	15.3	15.2

C. Test results and discussion

The experimental testing is conducted on In-Wheel type IPM motor. Test speed and torque are 1250rpm and 77.4Nm. The initial temperature is 25.2 degree and room temperature is 25 degree. Temperature sensors attached to the position of In-Wheel motor are shown in Fig. 7. Using total eight temperature sensors were tested and the results are shown in Fig. 10.

The temperatures of end-coil, housing, flange and permanent magnet is estimated. As a result of test, end-coil is saturated at 140 degree which is the highest temperature, housing at 87.2 degree and motor flange at 70.3 degree respectively. The end-coil, housing and flange reach saturation temperature in 3 hours and 30 minutes. TABLE III compares the experimental results and analysis results. It can be seen that the analyzed results have similar shape to the experimental and it is possible to predict the temperature of IPMSM. Using the predicted PM temperature, analysis of PM irreversible demagnetization can conduct.

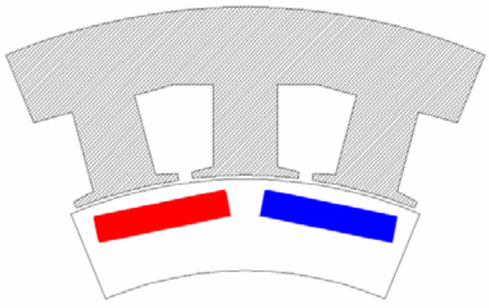

Fig. 6. Structure of IPMSM for in-wheel type EV

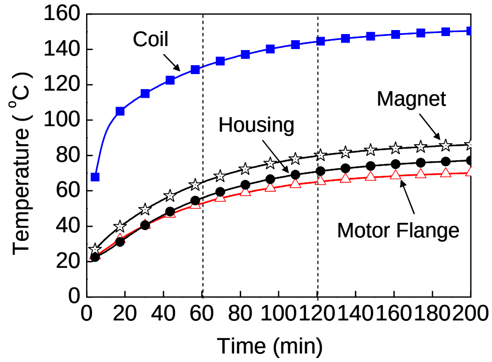

Fig. 9. Analysis results using thermal equivalent circuit of IPMSM

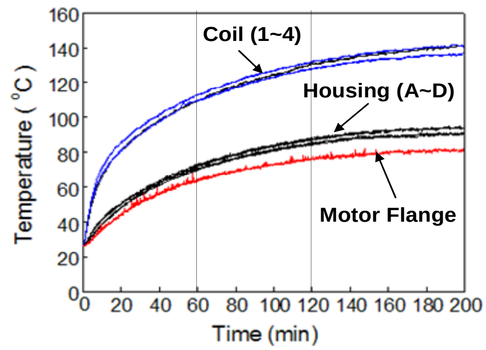

Fig. 10. Test results

IV. Conclusion

In this paper, a thermal equivalent circuit of IPMSM for estimating temperature is proposed. Using the numerical method, core losses at stator and rotor, and eddy current loss in PM are calculated. Compared with finite element thermal analysis, this equivalent circuit can solve the temperature of each motor component in shorter time. Therefore, it will be a very effective method to estimate the temperature of IPMSM in the design process. Also the analysis results using equivalent circuit of thermal is validated by a temperature test under load condition.

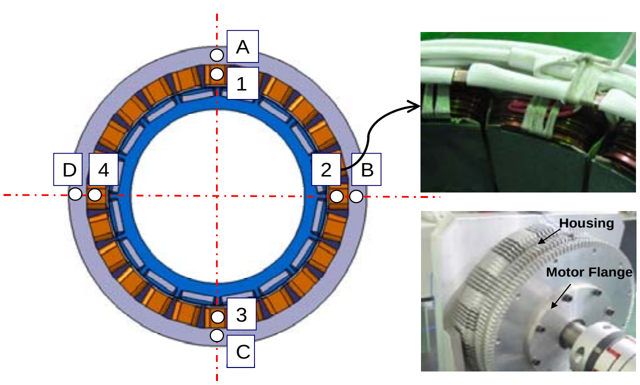

Fig. 7. Thermal sensor attached to the position of In-Wheel motor

Fig. 8. Test set

TABLE III
Comparison of Saturation Temperature

	End-coil	Housing	Magnet	Flange
Analysis[℃]	148	79.8	85.9	70.9
Test[℃]	140	87.2	-	70.3

References

[1] Ji-Young Lee, Sang-Ho Lee, Geun-Ho Lee, Jung-Pyo Hong, and Jin Hur, "Determination of Parameters Considering Magnetic Nonlinearity in an Interior Permanent Magnet Synchronous Motor", *IEEE Trans. on Magn.*, vol. 42, no. 4, pp.1303-1306, 2006.

[2] Jin Hur and Byeong-Woo Kim, " Rotor Shape Design of an Interior PM Type BLDC Motor for Improving Mechanical Vibration and EMI Characteristics", *JEET*, vol. 5, no. 3, pp.462-467, 2010.

[3] Kyung-Tae Kim, Kwang-Suk, Kim, Sang-Moon Hwang, Tae-Jong Kim, and Yoong-Ho Jung, " Comparison of Magnetic Forces for IPM and SPM Motor with Rotor Eccentricity", IEEE Transactions on Magnetics, Vol. 37, No. 5, pp.3448-3451, September 2001.

[4] G. H. Kang, J. P. Hong, G. T. Kim, J. W. Park, “Improved parameters modeling of interior permanent magnet synchronous motor by finite element analysis,” *IEEE Trans. on Magn.*, vol. 36, pp. 1867–1870, 2000.

[5] Lovatt, H. C., Watterson, P. A., “Energy stored in permanent magnets,” *IEEE Trans. on Magn.*, vol. 35, pp. 505–507, 1999.

[6] P. H. Mellor, D. R. Roberts, D. Turner, “Lumped Parameter Thermal Model For Electrical Machines of TEFC Design,” *IEE*, vol.138, no. 5, 1991.

[7] Kral, C., Habetler, T.G., Harley, R.G., Pirker, F., Pascoli, G., " Rotor temperature estimation of squirrel cage induction motors by means of a combined scheme of parameter estimation and a thermal equivalent model", *IEMDC*, 2003.

[8] Pinjia Zhang, Yi Du, Thomas G. Habetler, and Bin Lu, “Magnetic Effects of DC Signal Injection on Induction Motors for Thermal Evaluation of Stator Windings,” *IEEE Trans. on Industrial*, vol.58, no. 5, 2011.

[9] Seung-Hee Chai, Byeong-Hwa Lee, Jeong-Jong Lee, Jung-Pyo Hong, “Reduction Eddy Current Loss Design and Analysis of In-wheel type Vehicle Traction Motor”, *ICEM*, 2010

[10] S. O. Kwon, J. J. Lee, B. H. Lee, J. H. Kim, K. H. Ha, and J. P. Hong, “Loss Distribution of Three-Phase Induction Motor and BLDC Motor According to Core Materials and Operating,” *IEEE Trans. on Magn.*, vol. 45, no. 10, pp.4740-4743, 2009.

[11] Byeong-Hwa Lee, Soon-O Kwon, Tao Sun, Jung-Pyo Hong, Geun-Ho Lee, “Modeling of Core Resistance for d-q Equivalent circuit Aalysis of IPMSM considering Harmonic Linkage Flux”, *IEEE Trans. on Magn.*, vol. 47, no. 5, pp.1066 -1069, 2011.